First Principles Based Design and Experimental Evidence for a ZnO-Based Ferromagnet at Room Temperature

Marcel H. F. Sluiter,[1,*] Y. Kawazoe,[1] Parmanand Sharma,[1,†] A. Inoue,[1] A. R. Raju,[2] C. Rout,[2] and U. V. Waghmare[2]
[1]*Institute for Materials Research, Tohoku University, Sendai, 980-8577 Japan*
[2]*Jawaharlal Nehru Centre for Advanced Scientific Research, Jakkur, Bangalore, 560 064 India*
(Received 26 October 2004; published 12 May 2005)

The introduction of ferromagnetic order in ZnO results in a transparent piezoelectric ferromagnet and further expands its already wide range of applications into the emerging field of spintronics. Through an analysis of density functional calculations we determine the nature of magnetic interactions for transition metals doped ZnO and develop a physical picture based on hybridization, superexchange, and double exchange that captures chemical trends. We identify a crucial role of defects in the observed weak and preparation sensitive ferromagnetism in ZnO:Mn and ZnO:Co. We predict and explain codoping of Li and Zn interstitials to both yield ferromagnetism in ZnO:Co, in contrast with earlier insights, and verify it experimentally.

DOI: 10.1103/PhysRevLett.94.187204 PACS numbers: 71.23.−k, 71.55.Gs, 75.30.Hx, 85.30.De

For the emerging field of spintronics, it is essential to develop semiconductors with ferromagnetically polarized carriers at room temperature such that the spin as well as charge of the carriers can be coupled with an external magnetic field to control devices [1]. The design of dilute magnetic semiconductors (DMS) through minute substitution with a transition metal (TM) in III-V [2], II-VI [3], and IV [4] semiconductors has been pursued. For room temperature ferromagnetism, ZnO and GaN as host materials were predicted to be promising [2]. The experimental work on ZnO-based DMS following these predictions has been highly conflicting. The DMSs in ZnO:Co [5], ZnO:Ni [6,7], and ZnO:Mn [5,8,9] were found to be paramagnetic, while others reported ferromagnetism in at least some samples ZnO:Co [10–12], ZnO:Mn [13] both in bulk as well as in thin film form. Several recent studies on ZnO:Mn and ZnO:Co DMS showed that ferromagnetism depends strongly on methods and conditions used in the preparation [10,13,14]. Magnetic ordering in ZnO-based DMS appears sensitive to chemical ordering of the TM dopants and defects such as vacancies and interstitials. Spintronic applications [5,8] require that ferromagnetism has an intrinsic origin, i.e., not from magnetic TM atom clusters or impurity phases [15]. Through band structure arguments we analyze magnetic interactions and develop a general picture to understand their origin and trends that apply to other DMS systems also. Finally we confirm our predictions experimentally.

The magnetic couplings and the energetics of chemical ordering of ZnO with 5% substitution of Ti, V, Cr, Mn, Fe, Co, Ni for Zn were calculated using density functional theory (DFT) within the local spin density approximation (LSDA) [16] as implemented in the VASP package [17] with plane-wave ultrasoft pseudopotentials [18]. A periodic supercell (see Fig. 1) with 40 formula units of ZnO was used in all DFT calculations and two Zn atoms were replaced with TM atoms of one type at a time giving 10 distinct pairs of TM atoms. For each configuration, both ferromagnetic (FM) and antiferromagnetic (AFM) electronic configurations were calculated. The magnetic coupling for the pair of TM atoms is obtained from the FM and AFM total energy difference while a comparison of the density of states (DOS) gauges the significance of superexchange and double exchange for stabilizing AFM and FM configurations. We verified that structural optimization at fixed unit cell dimensions has little effect on the electronic structure and the couplings for ZnO:Co.

A qualitative understanding of the couplings is obtained through comparison of the AFM and FM DOS with that of the randomly polarized state (RND) using a hybridization picture; see Fig. 2. In Fig. 2(a) and 2(c) double (super) exchange between two FM (AFM) aligned TM atoms is shown schematically. The approximate tetrahedral symme-

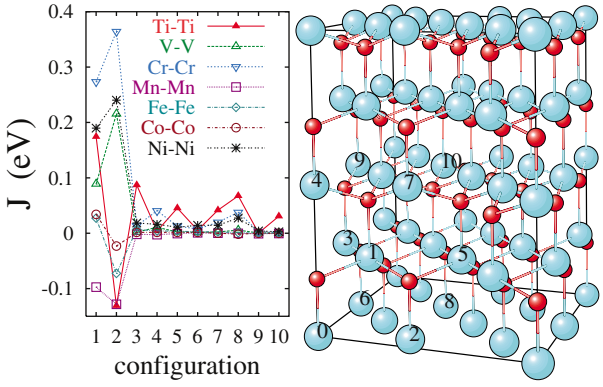

FIG. 1 (color). (left) Magnetic coupling J between substitutional TM atom pairs formed by site 0 and site N, labeled on the x axis and in the Wurzite ZnO supercell (right) where large blue (small red) spheres designate Zn (O) atoms. In the supercell the directions through atoms 1 and 3, 1 and 5, and 0 and 4 correspond to ⟨100⟩, ⟨010⟩, and ⟨001⟩, respectively. Positive J favor FM alignment.

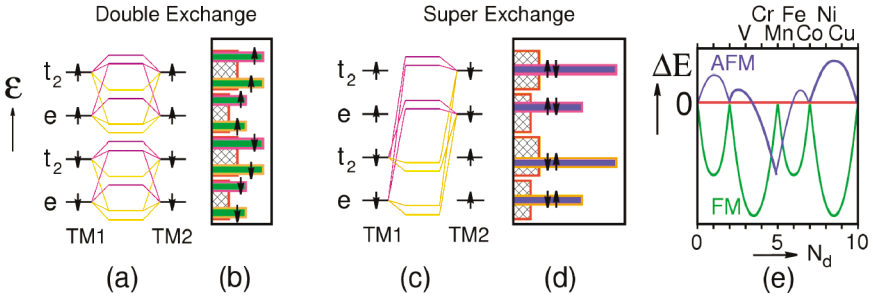

FIG. 2 (color). Schematic overview of hybridization and density of states in the case of (a), (b) direct exchange and (c), (d) super exchange interaction and resulting energetics of FM and AFM coupling between dopant atoms TM1 and TM2 relative to the random state (e).

try around the Zn/TM atoms causes the d-like levels to exhibit two and threefold degeneracies with e and t_2 character. The crystal field splitting in a spin channel is largest when it is partially filled and our computed DOS show that the exchange splitting is larger than the crystal field splitting. In ZnO the isolated TM atoms thus have levels e-spin-down, t_2-spin-down, e-spin-up, and t_2-spin-up from low to high energy. Hybridization for AFM is most significant for half d-band filling because of superexchange. Bonding (antibonding) hybrids are colored orange (purple). In Fig. 2(b) and 2(d) schematic DOS of FM (green), AFM (blue), and RND (red border, hatched) are shown. RND has the widest spread around each isolated-TM-atom level (subband) because it represents all possible local environments. The bonding (orange border) and antibonding (purple border) levels are far separated within each subband for FM. Therefore, when a given subband is half occupied FM is favored over RND. Hybridization is advantageous for AFM only near half band filling; therefore, only the central two AFM subbands deviate from the centers of the corresponding RND subbands. The two central AFM subbands are farther apart than the centers of the RND subbands because at half d-band filling, spin channels are completely full and completely empty making for optimal superexchange coupling. Figure 2(e) shows the band energy of FM and AFM relative to RND. FM is degenerate with RND whenever a subband is completely empty or completely filled, but at half filling FM is always lower in energy than RND because of the separation of bonding and antibonding levels per subband. At very low band filling AFM is not favored over RND because the latter has wider subbands so that initially lower energy levels are filled. When the lowest subband (e) is completely filled AFM and RND are energetically degenerate because hybridization with the much higher energy levels is weak. When the second subband (t_2) is filled, superexchange comes into play and AFM is much favored over RND. When the next subband is filled, the relative energy of AFM antibonding levels again makes AFM and RND degenerate. Hence, FM and AFM coupling are favored at specific d electrons per TM atom ratios (N_d). FM is favored over RND when $N_d = 1, 3.5, 6, 8.5$ while AFM occurs for $N_d = 5$. For $N_d = 2, 4, 6, 7$ details of the electronic structure play a role in FM-AFM competition. This simple picture applies to TM in ZnO (Fig. 2) where V^{2+}, Ni^{2+}, Cu^{2+} have FM nearest neighbors, Mn^{2+} has AFM nearest neighbors, while Fe^{2+} and Co^{2+} are of mixed type, and Cr^{2+} is FM. Figure 1 shows marked anisotropy in the nearest neighbor couplings (0-1, 0-2) consistent with the anisotropic oxygen-cation tight-binding parameters [19] and with recent experiments [20].

Longer-ranged interactions oscillate for Co and decay rapidly for Fe, indicative of the competing AFM and FM tendencies within our picture. Fitting a generalized RKKY form [21] to the calculated couplings revealed many choices of parameters which give fits of comparable quality but characteristic oscillations in the coupling versus distance are absent except for Co. We suggest that long-ranged coupling within LSDA, even in the absence of defects, is also readily explained by our hybridization picture of super and double exchange where the interaction is mediated not by oxygens but by delocalized Zn s-like states. These couplings, which are more relevant in the dilute limit [22], are usually thought of as carrier mediated deriving from the interaction $(S_i \cdot \sigma_j)$, where S_i (σ_j) is a spin of a TM d electron (carrier). Integrating out σ_j leads to long-ranged quadratic FM interaction [22] between S_i just as one would expect from our double exchange hybridization picture. However, for Mn we calculate a small but consistently AFM long-ranged coupling indicating that superexchange should not be neglected. It should be noted that the AFM state cannot be obtained in the single site coherent potential approximation [23]. Concerning a comparison with the polaron model, in the polaron model as presented in Fig. 4 of Ref. [20], the splitting of the d-like TM dopant states into e and t_2 subbands does not play an essential role although both the current model and the polaron model rely on delocalized electronic states for long-ranged coupling.

Based on the first-principles results and insights (Figs. 1 and 2), Ni and Cr (Ti) substitutions at all (low) concentrations are promising for ferromagnetism. Practical considerations make these TMs less suitable: Ni differs about 8% in Shannon-Previtt radius with Zn and is known to be poorly soluble in ZnO, while Cr and early TM do not usually take fourfold coordination in the 2+ oxidation state.

Total energies of Ni (Cr) substitution bear this out: the energy for the nearest neighbor configuration is about 0.34 (0.41) eV lower in energy than that for substitution at further distance indicating that Ni and Cr are likely to segregate and form clusters. Our analysis suggests that FM DMSs with Mn, Fe, or Co substitution are difficult to achieve without further modification. For concentrations above about 8%, nearest neighbor interactions become relevant and our results indicate that Mn and Fe substitution cannot result in FM and may exhibit glassy behavior [8].

As FM ZnO:TM remains contested, we probed if common native defects such as oxygen vacancies, zinc interstitials, and zinc vacancies could alter the magnetic interactions. DFT calculations with oxygen vacancies in the case of Co and Mn revealed little effect on the magnetic couplings because the induced donor state is too deep to significantly affect the occupancy of the extended TM levels. In contrast, both Zn interstitials and Zn vacancies change the occupancy of extended TM levels. Figure 2 indicates that both electron doping with zinc interstitials and hole doping with zinc vacancies make ZnO:Co and ZnO:Mn strongly FM. A recent experiment which showed that zinc interstitials make ZnO:Co FM [24] supports this finding. The important role played by Zn vacancies and Zn interstitials explains why preparation methods involving high temperatures fail to find FM in ZnO:Co and ZnO:Mn because under such conditions the Zn vacancies and Zn interstitials are generally lost and replaced with inert oxygen vacancies.

Our prediction that both hole doping *and* electron doping promote FM in ZnO:Co and ZnO:Mn is in marked contrast to some other DFT based predictions where only electron (hole) doping enhances FM in ZnO:Co (ZnO:Mn) [23] while in Ref. [25] hole doping only promotes FM in both ZnO:Co and ZnO:Mn. Interestingly, as expected from Fig. 2(e) both Lee *et al.* [26] and Spaldin [25] calculated that hole doping promotes FM coupling in ZnO:Co and recently it was experimentally observed [27], in contrast with Ref. [23].

As Co is highly soluble in ZnO [28], we decided to design a ZnO:Co based FM DMS by codoping. Our analysis suggests Li and In are good candidates as codopants based on matching ionic radii. We choose Li substitution for Zn because it does not have its own d electrons to interfere with magnetic ordering and it contradicts the previous DFT calculations [23], proving to be a good test of our picture. The number of configurations of relative positions of Li and two Co atoms is large and we restrict ourselves to the following cases: (1) two Co atoms with an intermediate or neighboring Li atom, (2) two Co atoms with a distant Li atom, and (3) two Co atoms with a distant interstitial Li with Zn vacancy. The former was found to be most energetically favorable, while the latter was least favorable. Surprisingly, in all three cases we find that Li amplifies the couplings between Co pairs, and for distant pairs the FM couplings are much enhanced. While the distant interactions remain weak (10 meV and less) their large number results in FM dilute ZnO:Co. Finite-temperature Monte Carlo simulations of ZnO:Co and ZnO:Co + Li using a classical Heisenberg model [22,29] with LSDA-determined neighbor couplings shows (see supplementary material [30]) that Li codoping promotes the FM state in ZnO:Co. As the spins randomly occupy Zn sites in the wurtzite crystal, the disorder enters these simulations through a random number of neighbors within the first ten neighbor shells with predetermined couplings. Behavior of ZnO:Co is found to be glassy at low temperatures for all concentrations considered while ZnO:Ni and ZnO:Co + Li are predicted to be FM up to temperatures approaching room temperature.

We find that Li_{Zn} induces a nonspin polarized s-like state with a radius of several angstroms. Moreover, electron deficiency at oxygens neighboring Li causes a charge transfer from electrons at the Fermi level associated with minority spin of late TMs, thus increasing the local moments of late TMs. Li codoping promotes long-ranged FM coupling as it brings the d electron/TM closer to the optimal values for double exchange not only for Co dopants but also for V and Cu dopants.

To verify our prediction we carried out experiments with various concentrations of Li and Co substitution in ZnO ($Zn_{1-x-y}Li_xCo_yO$). Zinc acetate, lithium acetate, and cobalt nitrate (Merk Extra pure $>99\%$ pure chemicals) are dissolved in the required molar ratio in double distilled water, and citric acid is added in 5:1 weight ratio. Under continuous stirring, the pH of the solution is adjusted to 7 to 7.5 by titrating ammonia. While stirring, the solution is heated to 350 K for 4 h and a thick transparent gel forms. The gel is dried at 450 K for 12 h and xerogel is obtained. This xerogel is heated in air at 673 K for 30 min to remove carbon and to form the required compounds as powders. The rather low-temperature synthesis is of significance [31] because we predict O vacancies to be detrimental to FM coupling. X-ray diffraction measurements of Li and Co substituted ZnO reveal no additional peaks in comparison with pure ZnO. The substitutional nature of Li doping is indicated by the linearly decreasing (increasing) lattice parameter **a** (**c**) with Li concentration at constant Co. The TEM examinations show a uniform particle size distribution around 50 nm without indications for other phases.

A Quantum Design MPMS-5S SQUID magnetometer was used for magnetic characterization in the temperature range from 5 K to 310 K. Magnetization hysteresis loops at 300 K and 10 K were measured by cycling the magnetic field between -1 T and $+1$ T and repeated at room temperature with a Lake Shore Vibrating Sample magnetometer VSM 7300. The change in hysteresis behavior in 5% Co-doped ZnO clearly shows (Fig. 3) that the FM (paramagnetic) component increases (decreases) with increasing Li concentration x. Measured remanent magnetization (Mr) as a function of x (Fig. 3 inset) confirms the onset of

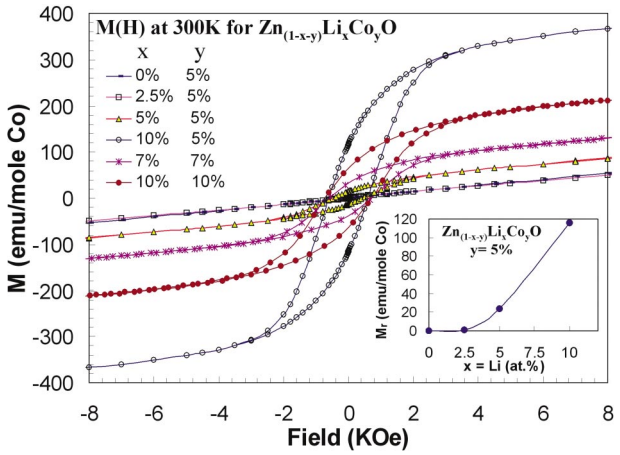

FIG. 3 (color). Hysteresis loops at 300 K for $Zn_{(1-x-y)}Li_xCo_yO$ powder. Inset shows remanent magnetization as function of Li concentration in 5% Co-doped ZnO.

FM with Li cosubstitution with a rapid increase in Mr from $x = 0.025$ to $x = 0.1$, while pure ZnO:Co is found not to be FM even up to $y = 0.1$. Comparison of samples with 5% and 10% Co (each with 10% Li) shows that ferromagnetism reduces with increasing concentration of Co, limited by the nearest neighbor AF interactions.

From the insights obtained from first-principles electronic structure of TM-substituted ZnO, we have developed a simple and general picture based on hybridization, superexchange, and double exchange that captures trends for the TM series in the short- and long-ranged magnetic interactions in DMS. Long-range interactions necessary for FM in DMSs can be mediated by defect induced states. Our picture successfully resolves the controversies reported for the occurrence of ferromagnetism in ZnO:Co and ZnO:Mn DMSs. We have theoretically argued that Co has the best potential as a Zn substitutional dopant in ZnO for producing DMS when combined with a hole dopant such as Li_{Zn} or an electron dopant such as Cu_{Zn} or interstitial Zn. SQUID measurements on low-temperature sol-gel synthesized samples confirm this prediction and demonstrate that room temperature ferromagnetism arises in ZnO:Co through hole doping with Li.

Part of this work was performed under the interuniversity cooperative research program of the Laboratory for Advanced Materials, IMR. M. H. F. S., Y. K., and U. V. W. thank the CCMS at IMR for allocations on the Hitachi SR8000 supercomputer system. U. V. W. thanks R. Seshadri for discussions and IMR for hospitality. Authors from JNCASR thank Professor C. N. R. Rao for comments and for research facilities. The authors thank R. C. Budhani for initial SQUID measurements and K. V. Rao and E. Kaxiras for comments on the manuscript.

*Lab. Mat. Sci., Delft Univ. Techn., 2628AL Delft, the Netherlands.

†Japan Science and Technology Agency, Sendai, Japan.

[1] S. A. Wolf *et al.*, Science **294**, 1488 (2001).
[2] T. Dietl, H. Ohno, F. Matsukura, J. Cibert, and D. Ferrand, Science **287**, 1019 (2000).
[3] A. Haury *et al.*, Phys. Rev. Lett. **79**, 511 (1997).
[4] L. Hansen *et al.*, Appl. Phys. Lett. **79**, 3125 (2001).
[5] G. Lawes, A. S. Risbud, A. P. Ramirez, and R. Seshadri, Phys. Rev. B **71**, 045201 (2005); C. N. R. Rao and F. L. Deepak, J. Mater. Chem. **15**, 573 (2005).
[6] Y. D. Park *et al.*, Science **295**, 651 (2002).
[7] K. Ando, Appl. Phys. Lett. **82**, 100-102 (2003).
[8] T. Fukumura *et al.*, Appl. Phys. Lett. **78**, 958 (2001).
[9] A. S. Risbud, N. A. Spaldin, Z. Q. Chen, S. Stemmer, and R. Seshadri, Phys. Rev. B **68**, 205202 (2003).
[10] K. Ueda, H. Tabata, and T. Kawai, Appl. Phys. Lett. **79**, 988 (2001).
[11] H.-J. Lee, S.-Y. Jeong, C. R. Cho, and C. H. Park, Appl. Phys. Lett. **81**, 4020 (2002).
[12] W. Prellier, A. Fouchet, B. Mercey, Ch. Simon, and B. Raveau, Appl. Phys. Lett. **82**, 3490 (2003).
[13] P. Sharma *et al.*, Nat. Mater. **2**, 673 (2003).
[14] J. H. Park, M. G. Kim, H. M. Jang, and S. Ryu, Appl. Phys. Lett. **84**, 1338 (2004).
[15] D. C. Kundaliya *et al.*, Nat. Mater. **3**, 709 (2004).
[16] J. P. Perdew and A. Zunger, Phys. Rev. B **23**, 5048 (1981).
[17] G. Kresse and J. Furthmüller, Phys. Rev. B **54**, 11169 (1996).
[18] D. Vanderbilt, Phys. Rev. B **41**, R7892 (1990).
[19] N. A. Hill and U. Waghmare, Phys. Rev. B **62**, 8802 (2000).
[20] M. Venkatesan, C. B. Fitzgerald, J. G. Lunney, and J. M. D. Coey, Phys. Rev. Lett. **93**, 177206 (2004).
[21] L. M. Roth, H. J. Zeiger, and T. A. Kaplan, Phys. Rev. **149**, 519 (1966).
[22] R. N. Bhatt, M. Berciu, M. P. Kennett, and X. Wan, J. Supercond. **15**, 71 (2002).
[23] K. Sato and H. Katayama-Yoshida, Phys. Status Solidi B **229**, 673 (2002).
[24] D. A. Schwarz and D. R. Gamelin, Adv. Mater. **16**, 2115 (2004).
[25] N. A. Spaldin, Phys. Rev. B **69**, 125201 (2004).
[26] E. C. Lee and K. J. Chang, Phys. Rev. B **69**, 085205 (2004).
[27] H.-T. Lin *et al.*, Appl. Phys. Lett. **85**, 621 (2004).
[28] V. Jayaram, J. Rajkumar, and B. Sirisha Rani, J. Am. Ceram. Soc. **82**, 473 (1999).
[29] L. Bergqvist, O. Eriksson, J. Kudrnovsky, V. Drchal, P. Korzhavyi, and I. Turek, Phys. Rev. Lett. **93**, 137202 (2004).
[30] See EPAPS Document No. E-PRLTAO-94-008521 for a figure that shows the calculated inverse magnetic susceptibility as a function of temperature for doped ZnO. A direct link to this document may be found in the online article's HTML reference section. The document may also be reached via the EPAPS homepage (http://www.aip.org/pubservs/epaps.html) or from ftp.aip.org in the directory /epaps/. See the EPAPS homepage for more information.
[31] P. Sharma, A. Gupta, F. J. Owens, A. Inoue, and K. V. Rao, J. Magn. Magn. Mater. **282**, 115 (2004).